

Synthesis of MCM-41 type materials with remarkable hydrothermal stability from UTM-1

Ziyu Liu, Yingxu Wei, Yue Qi, Shigang Zhang, Ying Zhang, Zhongmin Liu *

Applied Catalysis Laboratory, Dalian Institute of Chemical Physics, Chinese Academy of Sciences, 457 Zhongshan Road, Dalian 116023, PR China

Received 27 December 2005; received in revised form 13 February 2006; accepted 15 February 2006

Abstract

A microporous zeolite UTM-1 was prepared and transferred to MCM-41 type materials by refluxing with surfactant at the presence of NaOH and by a subsequent pH adjusting process. The pH value affected the long-range order of these mesostructures greatly, and MCM-41 type products were obtained at pH = 7 and pH = 5 (designated as MS-7 and MS-5, respectively). The as-synthesized MS-7 showed smaller particle sizes (about 500 nm) and cylindrical pores. MS-7 showed a high BET specific surface area of 1003 m²/g and a high pore volume of 1.20 cm³/g after calcination at 823 K as well as two pore size distributions centred at 2.4 and 3.7 nm, respectively. The calcined MS-7 exhibited remarkable hydrothermal stability. After being treated in boiling water for 312 h, the material remained a high BET specific surface area of 922 m²/g and a high pore volume of 1.08 cm³/g without degrading its well-ordered mesostructure. Compared with MS-7, the 823 K calcined MCM-41 showed poor hydrothermal stability and preserved only a BET specific surface area of 150 m²/g and a pore volume of 0.35 cm³/g upon being treated in boiling water for 24 h. The remarkable hydrothermal stability of MS-7 was ascribed by solid-state NMR results to the presence of higher percentage of 4-fold coordinated Al species and the highly polymerized pore walls.

© 2006 Elsevier Inc. All rights reserved.

Keywords: UTM-1; Post-synthetic treatment; pH adjusting; Mesoporous; Hydrothermal stability

1. Introduction

Silica-based MCM-41 type materials are potentially useful as sorbents, heterogeneous catalysts and catalyst supports [1]. However, these mesostructures usually collapsed after being treated in boiling water for just 24 h [2]. The poor hydrothermal stability hindered their practical applications severely since water is the most widely used medium in industry.

Several techniques have been developed to increase the hydrothermal stability of these MCM-41 type materials, including graft of Al onto pure siliceous materials [3], removal of silanol groups by silylation [4,5], preparation of materials with thicker pore walls [6,7], enhancement of

the condensation of silanol groups by salt effect [8–10] and/or by post-synthetic hydrothermal restructuring in water [11]. Among these techniques, graft of Al and increasing the condensation of silanol groups were effective to improve the hydrothermal stability, and the resulting material could remain stable after being treated in boiling water for 120 h [10]. Despite these improvements, the hydrothermal stability of silica-based MCM-41 type materials remains still inferior to that of microporous zeolites. Recently, the synthesis of silica-based MCM-41 type materials through seed solutions has drawn much attention [12–17]. That is, the synthesis of microporous zeolites, such as Y [12], beta [13–16] or ZSM-5 [13,17] was stopped after a period of crystallization to obtain clear solutions. These clear solutions contained primary structure units of corresponding microporous zeolites and were such called seed solutions. Then the seed solutions were used as silica sources to synthesize hydrothermally stable mesoporous

* Corresponding author. Tel.: +86 411 84685510; fax: +86 411 84691570.

E-mail address: Liuzm@dicp.ac.cn (Z. Liu).

materials. By this method, a MCM-41 type material named MAS-5 was prepared, which remained mesoporous after being treated in boiling water for 300 h [15]. The primary structure units were believed to be responsible for the extraordinary hydrothermal stability. But this method will be limited in case seed solutions are not available. In those circumstances, synthesis of hydrothermally stable MCM-41 type materials directly from microporous zeolites will be valuable and merit great efforts. UTM-1, possessing the same primary structure units as those of ZSM-5 [18], is a potential microporous zeolite for preparing hydrothermally stable mesoporous materials. Up to now, however, no study reported the possibility of synthesizing MCM-41 type materials with high hydrothermal stability from UTM-1.

In this study, synthesis is carried out by a two-step method, i.e., the preparation of precursor UTM-1 and then transferring it to MCM-41 type materials by refluxing with surfactant at the present of NaOH and by a subsequent pH adjusting process. The dependence of the mesostructures on pH values during the synthesis and the hydrothermal stability of the obtained mesoporous materials are investigated.

2. Experimental

2.1. Synthesis

Precursor UTM-1 was prepared as follows: 0.4 g of sodium aluminate (44.7 wt% Al_2O_3 , 39.2 wt% Na_2O), 2 g of NaOH and 2.16 g of NaCl were dissolved in 432 g of deionized water. To this solution, 32 g of fumed silica and 32 g of hexamethyleneimine (HMI) were added under stirring. The obtained mixture was heated in an autoclave at 423 K for 192 h with 90 r/min rotation. After being cooled to room temperature, the resulting solid was centrifuged, washed with deionized water and dried at 373 K overnight. To obtain mesostructured materials by post-synthetic treatments, 3 g of UTM-1 was dispersed in 315 g of deionized water containing 7.5 g of hexadecyltrimethylammonium bromide (CTAB) and 6.65 g of NaOH. After being refluxed at 373 K for 8 h and cooled to room temperature, the pH value of the obtained clear solution was adjusted using 2 M HCl solution to 9, 7, 5, 3, respectively. The resulting mixtures were stirred at room temperature for 12 h followed by centrifugation, washing and drying. The products were denoted as MS- n ($n = 9, 7, 5, 3$), where n denotes the final pH value.

For comparison, MCM-41 with similar Al content was synthesized using tetraethylorthosilicate (TEOS) as the starting material. A gel with the composition of TEOS: AlCl_3 :CTAB:NaOH:H₂O = 1:0.01:0.12:0.2:100 was transferred into an autoclave and crystallized statically at 393 K for 48 h. After being cooled to room temperature, the resulting solid was centrifuged, washed with deionized water and dried at 373 K overnight.

Calcination was carried out at 823 K for 10 h in a flow of air to remove the surfactant completely. In order to distinguish the samples calcined or not, the compound expres-

sion “as-synthesized” was used to refer to the samples containing surfactant and without calcination. The hydrothermal stability of these materials was investigated by treating the calcined samples in boiling water for different hours with the water to solid ratio of 100 ml/g.

2.2. Characterization

Powder X-ray diffraction (XRD) patterns were recorded on a D/Max-b X-ray diffractometer with Cu $K\alpha$ radiation of wavelength $\lambda = 0.15406$ nm (40 kV, 40 mA). Chemical compositions were obtained by X-ray fluorescence (XRF) method on a Philips Magix X spectrometer. Fourier transform infrared spectroscopy (FTIR) studies were performed on a Bruker EQUINOX 55 spectrometer by KBr pellet method. The spectra were acquired in the range between 400 and 4000 cm^{-1} at 4 cm^{-1} resolution and 32 scans. Scanning electron microscopy (SEM) images were taken with a KYKY-AMRAY-1000B electron microscope. Transmission electron microscopy (TEM) studies were carried out with a JEOL JEM-2000Ex electron microscope with an accelerating voltage of 120 kV. Nitrogen adsorption isotherms were measured at 77 K on a NOVA 4000 volumetric adsorption analyzer. Prior to the measurements, the samples were outgassed at 623 K for at least 4 h. The specific surface area was calculated by the Brunauer–Emmett–Teller (BET) method [19]. The total pore volume was determined from the amount adsorbed at a relative pressure of about 0.99. The pore size distributions were calculated from desorption branches of nitrogen isotherms using the Barrett–Joyner–Halenda (BJH) model [19]. Solid-state ^{27}Al MAS NMR spectra were obtained on a Varian InfinityPlus 400 spectrometer equipped with a 4 mm zirconia rotor (8 kHz spin rate) operating at 104.17 MHz and 2.0 s of pulse delay with a spectral width of 40.0 kHz. Solid-state ^{29}Si MAS NMR spectra were obtained on the same spectrometer equipped with a 7.5 mm zirconia rotor (4 kHz spin rate) operating at 79.42 MHz and 8.0 s of pulse delay with a spectral width of 35.0 kHz. The chemical shifts of ^{27}Al and ^{29}Si (in ppm) were externally referenced to $[\text{Al}(\text{H}_2\text{O})_6]^{3+}$ aqueous solution and tetramethylsilane, respectively.

3. Results and discussion

XRD patterns of as-synthesized samples are shown in Fig. 1. The diffractions of the precursor (Fig. 1A) are identical to those reported [18], indicating a pure UTM-1 phase. After the post-synthetic treatment, the appearance of diffractions in low angle region and the disappearance of those in high angle region indicate that UTM-1 has been transferred to mesostructured materials with amorphous frameworks (Fig. 1B–E). But the pH value affects the ordering of these mesostructures significantly. MS-9 shows only a broad diffraction in low angle region implying a disordered mesostructure. However, decreasing the pH value to 7 results in three diffractions corresponding to d

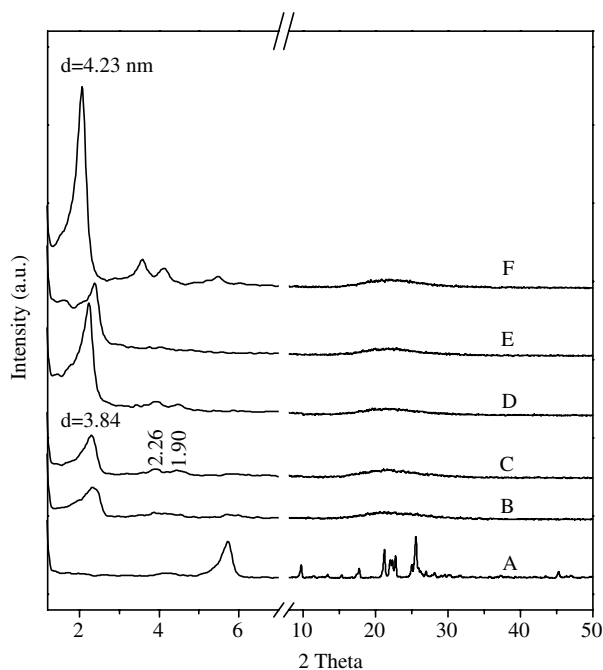


Fig. 1. XRD patterns of as-synthesized (A) UTM-1, (B) MS-9, (C) MS-7, (D) MS-5, (E) MS-3 and (F) MCM-41.

spacings of 3.84, 2.26 and 1.90 nm (Fig. 1C). These diffractions are comparable to those of MCM-41 (Fig. 1F) and can be indexed as (100), (110) and (200) of a hexagonal mesostructure. The lattice constant a_0 of MS-7 is 4.43 nm ($a_0 = 2 d_{(100)}/\sqrt{3}$), which is a little smaller than that of MCM-41 ($a_0 = 4.94$ nm). MS-5 also shows these three diffractions, and the (100) intensity is strengthened (Fig. 1D) implying an even more ordered mesostructure. Lowering the pH value further to 3, whereas, leads to a decreased (100) intensity and the vanishing of the (110) and (200) diffractions (Fig. 1E), showing that the long-range order of the mesostructure is degraded. At the same time, the a_0 of MS- n increases slightly from MS-9 to MS-5 as indicated by the (100) diffraction shifting to lower angles while the a_0 decreases sharply from MS-5 to MS-3. The changes in the long-range order and the lattice constant show that the pH values between 7 and 5 favor the formation of desirable mesostructures. The structural dependence of MS- n on the pH values may be related to the silica condensation rate. The rate must be sufficiently high so that the mesostructure can be locked in solid form, but must also be slow enough to accommodate the surfactant [20]. It was reported that the silica condensation rate was influenced greatly by pH values [21]. In our conditions, the pH values between 7 and 5 may lead to suitable silica condensation rate, which promotes the self-assembly between the surfactant and the silicate species, thus well-ordered mesostructures are obtained. It is found that the kind of precursors also affects the synthesis results. If MCM-22 is used as the precursor, only a very weak and broad XRD peak in the low angle region can be observed indicating a poor mesostructure.

Fig. 2 gives the SEM images of as-synthesized MCM-41 and MS-7. Both samples are spherically shaped and are uniform in particle size. MCM-41 shows a particle size of about 5 μm , however, the particle size of MS-7 is much smaller (about 500 nm). The smaller particle size of MS-7 may bring better catalytic and separation performance due to its accessibility of the active phase, especially where a higher reaction rate is required [22]. The difference in particle sizes of these two samples may be caused by the different synthesis conditions. MS-7 was synthesized under stirring at room temperature while MCM-41 was prepared hydrothermally at 393 K in static conditions. The combination of the lower synthesis temperature with the stirring conditions results in the smaller particle size of MS-7.

Fig. 3 shows typical TEM images of as-synthesized samples. Both MCM-41 (Fig. 3A) and MS-7 (Fig. 3B) exhibit arrays of parallel lines, indicating the formation of ordered structures. These parallel lines can be attributed to lamellar structures or cylindrical pores of hexagonal structures. The latter can be confirmed because the ordered structures remain after calcination at 823 K, as discussed below, while lamellar structures generally collapse at 623 K [23]. The pore length of MS-7 is shorter compared with that of MCM-41, which should be caused by its smaller particle size. The a_0 measured from TEM is 4.73 nm for MCM-41 and 4.45 nm for MS-7, these data agree well with the results from XRD (4.94 and 4.43 nm, respectively).

Fig. 4 illustrates the FTIR spectra of as-synthesized samples. For UTM-1 sample (Fig. 4A), the broad bands centered at about 3500 and 1641 cm^{-1} stem from the absorbed water on the surface. The bands at 3000–2800 and 1448 cm^{-1} come from the stretching and deformation vibrations of C–H, which originate from the HMI molecules occluded in this sample. The bands at 1217 and 789 cm^{-1} can be assigned to the stretching vibrations of Si–O–Si [24]. The band at 1094 cm^{-1} may be attributed to the Si–O stretching vibration [24]. The weak bands at 964 and 912 cm^{-1} can be ascribed to the stretching vibration of C–C and C–N from HMI, respectively [25]. The bands at 640–400 cm^{-1} may come from the five-membered rings in the primary structure units of UTM-1 [26]. After the post-synthetic treatment, the vibrations of C–H as well as those of C–C and C–N in MS-7 are strengthened (Fig. 4B), which is caused by the addition of CTAB. Surprisingly, the bands at the range of 640–400 cm^{-1} disappear, indicating that no primary structure units of UTM-1 remain in MS-7. The disappearance of the primary structure units of UTM-1 may be related to the complete dissolving of the precursor during the refluxing step, as indicated by the clear solution before the pH adjustment. Instead, the appearance of the broad band centered at 462 cm^{-1} as well as the similarity between the spectra of MS-7 and MCM-41 (Fig. 4C) confirms that the framework of MS-7 is amorphous, which agrees well with the results from Fig. 1.

The XRD patterns of 823 K calcined and subsequently boiling water treated samples are shown in Fig. 5, and

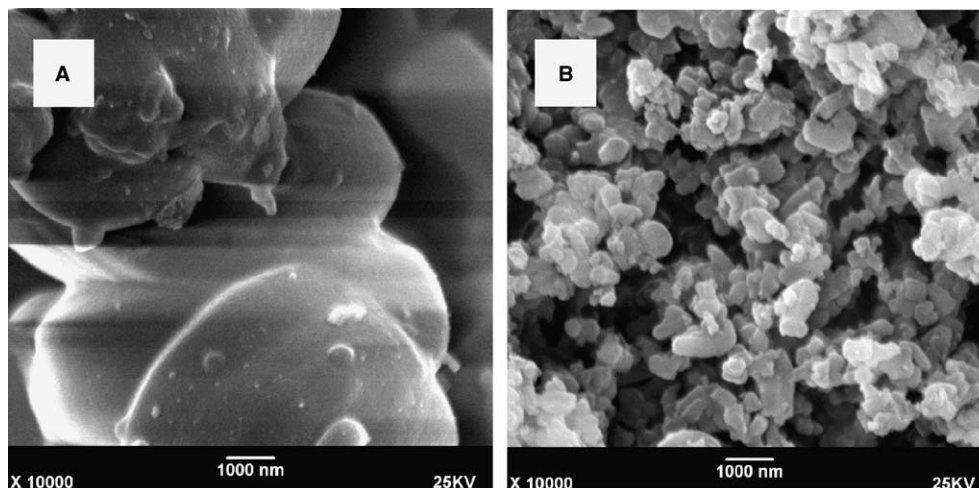


Fig. 2. SEM images of as-synthesized (A) MCM-41 and (B) MS-7.

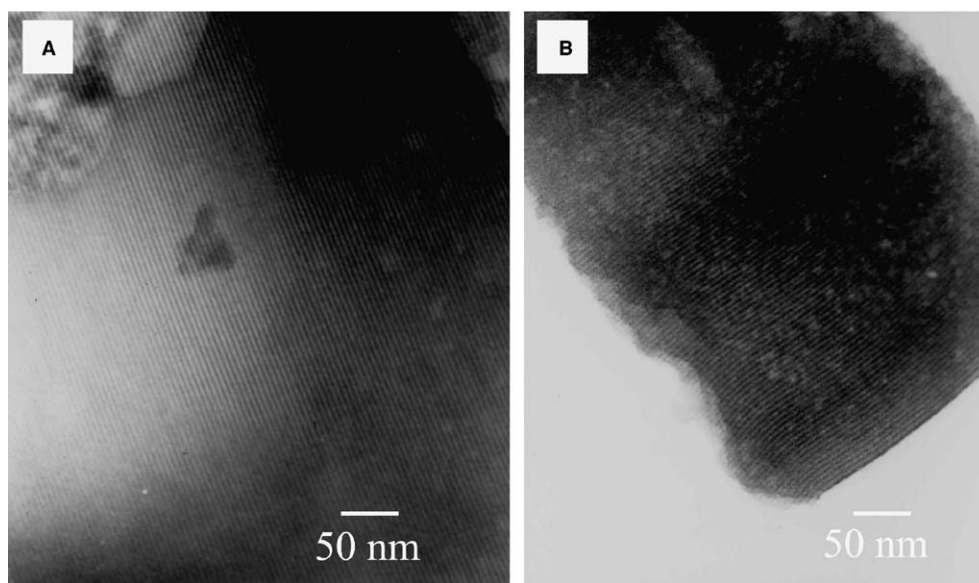


Fig. 3. TEM images of as-synthesized (A) MCM-41 and (B) MS-7.

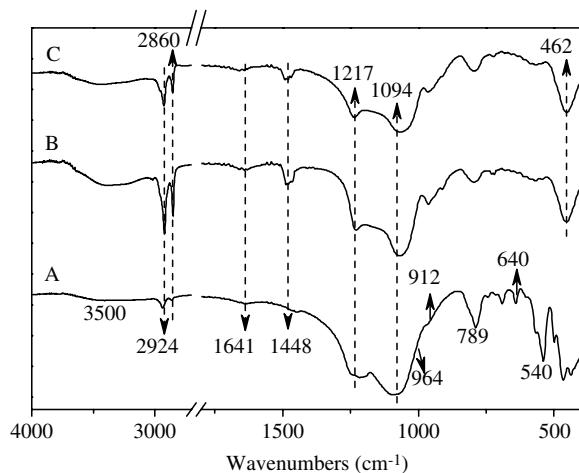


Fig. 4. FTIR spectra of as-synthesized (A) UTM-1, MS-7 and (C) MCM-41.

the corresponding d spacings and a_{0s} are listed in Table 1. Both MS-7 (Fig. 5A, a) and MCM-41 (Fig. 5B, a) remain all the hexagonal diffractions after calcination. No lattice shrinkage can be observed for MS-7 after calcination compared with the as-synthesized one while the a_0 of MCM-41 shrinks by 11%, indicating that the former is more thermally stable. After being treated in boiling water for 24 h, MS-7 preserves the well-ordered hexagonal structure with almost unchanged diffraction intensity. Increasing the time in boiling water up to even 312 h has no visible effect on the mesostructure of MS-7 (Fig. 5A, c–d). On the contrary, only the (100) diffraction with greatly weakened intensity remains for MCM-41 upon being treated in boiling water for just 24 h, and prolonging the treating time destroys the structure completely (Fig. 5B, b–d). These data verify that MS-7 is much more hydrothermally stable than MCM-41.

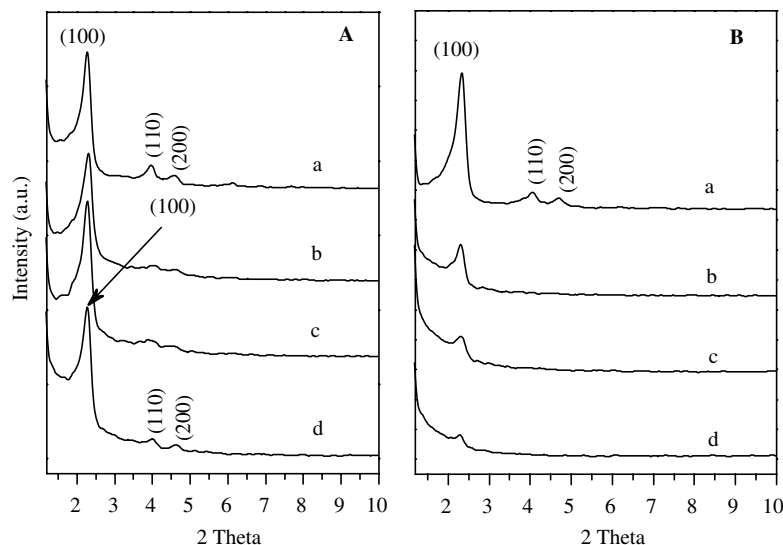


Fig. 5. XRD patterns of 823 K calcined (A) MS-7 and (B) MCM-41 after being treated in boiling water for (a) 0 h, (b) 24 h, (c) 120 h and (d) 312 h. The intensity scales are the same for these samples.

Table 1
Textural data of calcined and water treated samples

Sample	S_{BET} (m^2/g)	V_{p} (cm^3/g)	P_{PSD} (nm)	$d_{(100)}$ (nm)	a_0 (nm)	b (nm)
MS-7	1003	1.20	2.4	3.89	4.49	2.09
MS-7 ^a	922	1.08	2.2	3.89	4.49	2.29
MCM-41	858	0.68	2.2	3.79	4.38	2.18
MCM-41 ^b	150	0.35	3.8	3.83	4.42	0.62

S_{BET} , the BET specific surface area; V_{p} , pore volume; P_{PSD} , the pore diameter calculated using BJH method; b , wall thickness, $b = a_0 - P_{\text{PSD}}$.

^a After being treated in boiling water for 312 h.

^b After being treated for 24 h.

MS-7 and MCM-41 both exhibit type IV isotherms after the calcination (Fig. 6) indicating the formation of mesoporous structures, which agrees well with the XRD results. The isotherm of MS-7 shows a strong uptake of N_2 in a relative pressure (p/p_0) range of 0.25–0.35 due to capillary condensation, and a large hysteresis loop at p/p_0 range of 0.45–0.99 is also observed (Fig. 6A). This kind of isotherm indicates the presence of secondary mesopores [10], as proved by the two mesoporous pore size distributions centered at 2.4 and 3.7 nm, respectively (Fig. 6, inset A). Take into account that most of the pores are centred at 2.4 nm, this one is used to calculate the wall thickness and thus a wall thickness of 2.09 nm is obtained. Table 1 shows that MS-7 has a BET specific surface area of 1003 m^2/g and a pore volume of 1.20 cm^3/g . These data are comparable to those of silica-based mesoporous materials [27]. MCM-41, however, shows only one strong capillary condensation at p/p_0 range of 0.20–0.30 (Fig. 6B), indicating a uniform pore size distribution. The sample exhibits a BET specific surface area of 858 m^2/g and a pore volume of 0.68 cm^3/g (Table 1). The uniform pore size of MCM-41 is centred at 2.2 nm (Fig. 6, inset B) and a wall thickness of 2.18 nm can be inferred, which is similar to that of MS-7.

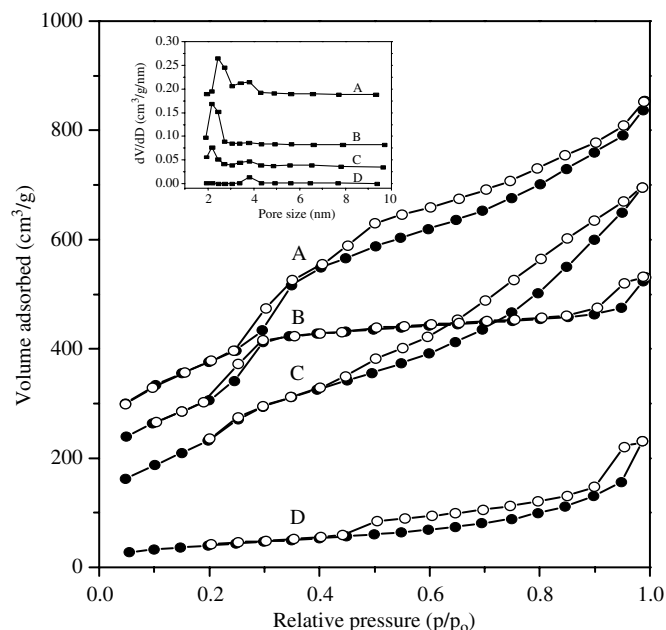


Fig. 6. N_2 adsorption isotherms of 823 K calcined MS-7 (A) and MCM-41 (B) as well as boiling water treated sample A for 312 h (C) and boiling water treated sample B for 24 h (D). Curve (A) and (B) are offset by 100 cm^3/g for clarity.

After being treated in boiling water for 312 h, the isotherm of MS-7 still shows a capillary condensation at p/p_0 range of 0.20–0.30 and the hysteresis loop at higher p/p_0 range also remains (Fig. 6C), indicating the existence of mesopores. The sample keeps a BET specific surface area of 922 m^2/g and a pore volume of 1.08 cm^3/g as well as two pore sizes of 2.2 and 3.7 nm. For the same reasons mentioned above, the wall thickness is estimate to be 2.29 nm. However, upon being treated in boiling water for 24 h, the isotherm of MCM-41 exhibits virtually no

capillary condensation (Fig. 6D), showing that the mesostructure of MCM-41 has collapsed, as implied by the very thin pore walls. Table 1 shows that the BET specific surface area and pore volume of the boiling water treated MCM-41 are reduced to 150 m²/g and 0.35 cm³/g, respectively.

The XRD patterns and N₂ adsorption measurements have experimentally evidenced that the hydrothermal stability of MS-7 is much higher than that of MCM-41. Since these two samples possess almost identical frameworks and comparable wall thickness, other factors should be responsible for the remarkable hydrothermal stability of MS-7. As described in the experimental part, the MCM-41 sample was synthesized through the conventional hydrothermal route since we could not manage to prepare well-ordered MCM-41 sample under the same conditions as those of MS-7. It seems that the difference between the synthesis conditions may bring about the different hydrothermal stability. However, though MCM-41 type materials have been prepared under various conditions in literatures [3–11], none of them showed a hydrothermal stability of more than 120 h in boiling water except those from seed solutions. So the remarkable hydrothermal stability of 312 h for MS-7 can hardly be caused by the different synthesis conditions.

Difference in the composition of mesostructures may also affect their hydrothermal stability. As detected by the XRF method, the as-synthesized UTM-1 sample exhibits a Si/Al ratio of 135, whereas, the ratio decreases to 88 for MS-7. This may be caused by that UTM-1 was dissolved during the refluxing step and then assembled into MS-7, during which the Al species were more readily incorporated into the MS-7 framework compared with the Si species. The Si/Al ratio of MCM-41 sample is 99, which is a little higher than that of MS-7. As discussed above, the latter (with the lower Si/Al ratio) shows much higher hydrothermal stability than MCM-41, which is somewhat different from the results of Bore et al. [28], who obtained lower hydrothermal stability when the Si/Al ratio is lower.

Solid-state ²⁷Al MAS NMR spectra of as-synthesized samples are shown in Fig. 7. Each of the samples exhibits a resonance centred at chemical shift of 52.4 ppm and a broad one around 13.4 ppm. The former comes from the 4-fold coordinated Al species while the latter is usually attributed to the 6-fold coordinated Al species [28–30]. It was reported [31] that the structural degradation of pure silica MCM-41 in water occurred due to the hydrolysis of siloxane (Si–O–Si) bonds and that the incorporation of Al created Si–O–Al bonds, which were more resistant to attack from water. Meanwhile, the presence of 4-fold coordinated Al species in MCM-41 type materials would create a negative charge on the framework, which repelled the OH[−] ions that catalyzed the hydrolysis of siloxane bonds [29]. Judging from this, increasing the amount of 4-fold coordinated Al species will increase the hydrothermal stability of MCM-41 type materials. In our cases, the percentages of the 4-fold coordinated Al species are 65.8%, 84.6% and 70.1% for UTM-1, MS-7 and MCM-41, respectively.

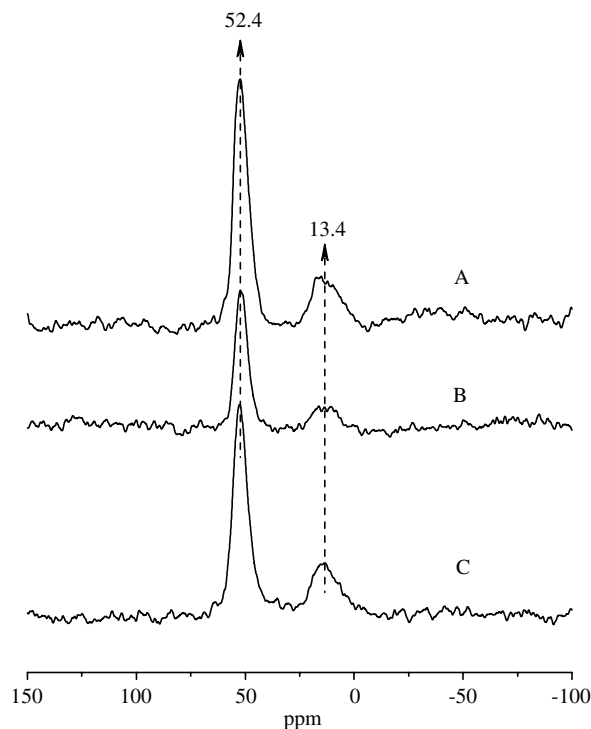


Fig. 7. ²⁷Al MAS NMR of as-synthesized (A) UTM-1, (B) MS-7 and (C) MCM-41.

The much higher percentage of the 4-fold coordinated Al species in MS-7 contributes to its remarkable hydrothermal stability.

Solid-state ²⁹Si MAS NMR spectra of as-synthesized samples are shown in Fig. 8. UTM-1 exhibits mainly one resonance at chemical shift of −103.3 ppm and another centred at −114.3 ppm (Fig. 8A). The former can be ascribed to Si(OSi)₃(OH) (Q³) and the latter to Si(OSi)₄ (Q⁴) framework units [32]. After the post-synthetic treatment, the resulting MS-7 shows three resonances centred at −92.1, −101.0 and −111.3 ppm (Fig. 8B), which are typical for silica-based mesoporous materials. These resonances can be attributed to Si(OSi)₂(OH)₂ (Q²), Q³ and Q⁴ framework units, respectively [33,34]. MCM-41 shows similar framework units as those of MS-7 (Fig. 8C), which agrees well with the FTIR results. Generally, the increase in the full condensation of the pore walls (Q⁴) will increase the hydrothermal stability of silica-based mesoporous materials and the ratio of Q⁴/Q³ or Q⁴/(Q³ + Q²) is often used to indicate the degree of condensation. The integral of Q⁴, Q³ and Q² as well as corresponding ratios of these samples are listed in Table 2. As can be seen, UTM-1 exhibits a Q⁴/Q³ ratio of 4.05 while MS-7 shows a lower value than that of UTM-1. This may be caused by the complete dissolution of the UTM-1 framework. Though the dissolved UTM-1 subsequently assembled with CTAB and formed MS-7 sample, only a less condensed framework was obtained in our experiments, which led to the lower Q⁴/Q³ ratio. However, both the Q⁴/Q³ and Q⁴/(Q³ + Q²) ratios of MS-7 are higher than those of MCM-41. The higher ratios indicate that the pore

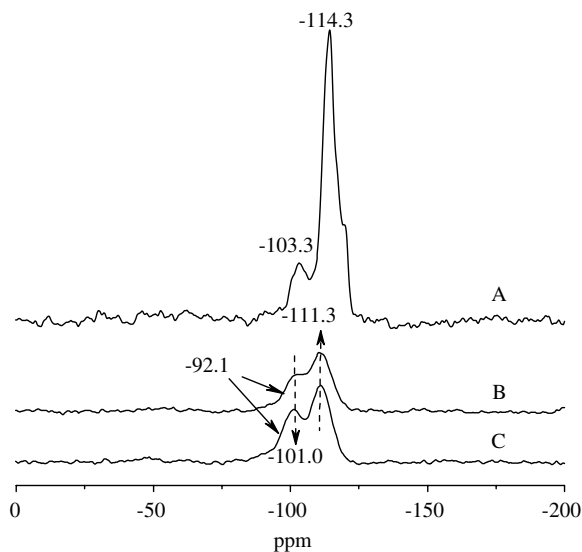


Fig. 8. ^{29}Si MAS NMR of as-synthesized (A) UTM-1, (B) MS-7 and (C) MCM-41.

Table 2
Parameters and corresponding ratios from ^{29}Si MAS NMR

Sample	Q^2 (%)	Q^3 (%)	Q^4 (%)	Q^4/Q^3	$Q^4/(Q^3 + Q^2)$
UTM-1	— ^a	19.42	78.70	4.05	— ^a
MS-7	4.44	34.12	61.44	1.80	1.59
MCM-41	5.53	38.84	55.63	1.43	1.25

^a No Q^2 can be detected.

walls are more polymerized in MS-7. Though the IR spectrum (Fig. 4) does not show clearly there are less amount of internal hydroxyls, the more polymerized pore walls of MS-7 can also be confirmed by the uncontracted a_0 upon calcination [35]. As a result, MS-7 shows much higher hydrothermal stability than MCM-41. Taking in account the results from ^{27}Al NMR, it is clear that the higher percentage of 4-fold coordinated Al species and the highly polymerized pore walls are responsible for the remarkable hydrothermal stability of MS-7 mesostructure.

4. Conclusions

In summary, using a simple dissolving and subsequent pH adjusting method, MCM-41 type materials can be synthesized from UTM-1. The obtained sample exhibited remarkable hydrothermal stability. After being treated in boiling water for 312 h, MS-7 remained a high BET specific surface area of $922\text{ m}^2/\text{g}$ and a high pore volume of $1.08\text{ cm}^3/\text{g}$ without degrading its well-ordered mesostructure. It was suggested that the higher percentage of 4-fold coordinated Al species and the highly polymerized pore walls be responsible for the remarkable hydrothermal sta-

bility. This method provides a possible way to synthesize ordered mesoporous materials from microporous zeolites.

References

- [1] A. Corma, Chem. Rev. 97 (1997) 2373.
- [2] J.M. Kim, R. Ryoo, Bull. Kor. Chem. Soc. 17 (1996) 66.
- [3] A.S. O'Neil, R. Mokaya, M. Poliakoff, J. Am. Chem. Soc. 124 (2002) 10636.
- [4] K.A. Koyano, T. Tatsumi, Y. Tanaka, S. Nakata, J. Phys. Chem. B 101 (1997) 9436.
- [5] X.S. Zhao, G.Q. Lu, J. Phys. Chem. B 102 (1998) 1556.
- [6] D. Zhao, J. Feng, Q. Huo, N. Melosh, G.H. Fredrickson, B.F. Chmelka, G.D. Stucky, Science 279 (1998) 548.
- [7] N. Coustel, F.D. Renzo, F. Fajula, J. Chem. Soc., Chem. Commun. (1994) 967.
- [8] R. Ryoo, S. Jun, J. Phys. Chem. B 101 (1997) 317.
- [9] J.M. Kim, R. Ryoo, J. Phys. Chem. B 103 (1999) 6200.
- [10] J. Yu, J.L. Shi, H.R. Chen, J.N. Yan, D.S. Yan, Micropor. Mesopor. Mater. 46 (2001) 153.
- [11] L.Y. Chen, T. Horiuchi, T. Mori, K. Maeda, J. Phys. Chem. B 103 (1999) 1216.
- [12] Y. Liu, W.Z. Zhang, T.J. Pinnavaia, J. Am. Chem. Soc. 122 (2000) 8791.
- [13] Y. Liu, W.Z. Zhang, T.J. Pinnavaia, Angew. Chem. Int. Ed. 40 (2001) 1255.
- [14] Z.T. Zhang, Y. Han, L. Zhu, R.W. Wang, Y. Yu, S.L. Qiu, D.Y. Zhao, F.-S. Xiao, Angew. Chem. Int. Ed. 40 (2001) 1258.
- [15] Z.T. Zhang, Y. Han, F.-S. Xiao, S.L. Qiu, L. Zhu, R.W. Wang, Y. Yu, Z. Zhang, B.S. Zou, Y.Q. Wang, H.P. Sun, D.Y. Zhao, Y. Wei, J. Am. Chem. Soc. 123 (2001) 5014.
- [16] Y. Han, F.S. Xiao, S. Wu, Y.Y. Sun, X.J. Meng, D.S. Li, S. Lin, F. Deng, X.J. Ai, J. Phys. Chem. B 105 (2001) 7963.
- [17] Y. Han, S. Wu, Y.Y. Sun, D.S. Li, F.S. Xiao, J. Liu, X.Z. Zhang, Chem. Mater. 14 (2002) 1144.
- [18] K. Yamamoto, J. Plévert, M. Uneme, T. Tatsumi, Micropor. Mesopor. Mater. 55 (2002) 81.
- [19] K.S.W. Sing, D.H. Everett, R.A.W. Haul, L. Moscou, R.A. Pierotti, J. Rouquerol, T. Siemienińska, Pure Appl. Chem. 57 (1985) 603.
- [20] M.T. Bore, S.B. Rathod, T.L. Ward, A.K. Datye, Langmuir 19 (2003) 256.
- [21] C.J. Brinker, J. Non-Cryst. Solids 100 (1988) 31.
- [22] L. Tosheva, V.P. Valchev, Chem. Mater. 17 (2005) 2494.
- [23] U. Ciesla, F. Schüth, Micropor. Mesopor. Mater. 27 (1999) 131.
- [24] Y.N. Huang, Z.M. Jiang, W. Schwieger, Chem. Mater. 11 (1999) 1210.
- [25] Q. Cai, C.P. Wei, R.Y. Xu, W.Q. Pang, K.J. Zhen, Chem. J. Chin. Univ. 20 (1999) 344.
- [26] E.G. Derouane, J. Weitkamp, J. Chem. Soc., Chem. Commun. (1981) 591.
- [27] C.T. Kresge, M.E. Leonowicz, W.J. Roth, J.C. Vartuli, J.S. Beck, Nature 359 (1992) 710.
- [28] M.T. Bore, R.F. Marzke, T.L. Ward, A.K. Datye, J. Mater. Chem. 15 (2005) 5022.
- [29] R. Mokaya, J. Phys. Chem. B 104 (2000) 8279.
- [30] K.M. Reddy, C.S. Song, Catal. Lett. 36 (1996) 103.
- [31] S.C. Shen, S. Kawi, J. Phys. Chem. B 103 (1999) 8870.
- [32] C.M. Leu, Z.W. Wu, K.H. Wei, Chem. Mater. 14 (2002) 3016.
- [33] R. Mokaya, J. Phys. Chem. B 103 (1999) 10204.
- [34] S. Inagaki, Y. Fukushima, K. Kuroda, Stud. Surf. Sci. Catal. 84 (1994) 125.
- [35] R. Mokaya, Chem. Commun. (2001) 933.